

Detection Scheme for PNC-Based Cell-Free MIMO Systems

İrem Cumalı*, Berna Özbek* and Güneş Karabulut Kurt†

*Department of Electrical and Electronics Engineering, Izmir Institute of Technology, Izmir, Türkiye

†Poly-Grames Research Center, Department of Electrical Engineering, Polytechnique Montréal, Montréal, Canada
{iremocal, bernaozbek}@iyte.edu.tr, gunes.kurt@polymtl.ca

Abstract—Cell-free multiple-input multiple-output (cell-free MIMO) is a promising concept to overcome inter-cell interference and avoid non-uniform data rates among users by combining the best features of ultra-dense networks and MIMO. Hence, cell-free MIMO can fulfill the increasing demand on data rate with uniformly good coverage for the sixth-generation (6G) wireless communications. In addition to that, physical-layer network coding (PNC) reduces the transmission delay since it requires only two time slots instead of four time slots to exchange information between two users. In this paper, we propose a novel scheme called PNC-based cell-free MIMO to improve reliability further while reducing the transmission delay. We demonstrate the effectiveness of the proposed scheme regarding the bit error rate in different system configurations. The proposed PNC-based cell-free MIMO achieves significantly lower error probability than the conventional cell-free MIMO.

Index Terms—Cell-free MIMO, physical-layer network coding, sixth-generation (6G) communications.

I. INTRODUCTION

The concept of small cells has gained importance over the years due to its capability to increase network capacity. However, deploying more small cells cannot enhance the capacity after a certain point due to the increasing inter-cell interference. On the other hand, the cell-edge users are exposed to significant interference, which leads to non-uniform data rates for the users within the cell. Hence, the idea of serving a small number of users with a massive number of ubiquitous access points (APs) has been reconstructed under the concept of cell-free MIMO to achieve uniform data rates while limiting the inter-cell interference for the sixth-generation (6G) communication systems.

The cell-free MIMO architecture in a canonical form has emerged in [1], [2] while providing three main benefits over the cellular networks: higher average signal-to-noise ratio (SNR) with lower variations, better ability to manage interference, and increased SNR through coherent transmission [3]. The reason for higher SNR with lower variations in cell-free MIMO is that the distance from the closest AP in the cell-free MIMO network is much shorter than that of the cellular MIMO network [4]. Furthermore, the cell-free MIMO experiences low variations in the signal-to-interference-plus-noise ratio (SINR), while the cellular MIMO system cannot ensure uniformly great service for each user within the cell [1]–[4]. Since multiple APs perform joint processing in the uplink, cell-free MIMO can cope with the interference better, which increases

the system data rate. Also, the coherent transmission in the downlink results in higher SNR.

Furthermore, the concept of cell-free MIMO exploits the features of MIMO, coordinated multi-point (CoMP), and ultra-dense networks so that it can be evaluated as the intersection of these technologies [5]. However, it should be noted that cell-free MIMO is a scalable version of network MIMO or coordinated multi-point joint transmission (CoMP-JT) and mainly aims to serve both the cell-edge users and cell-center users uniformly while minimizing the fronthaul load [4], [6]. Thus, this paper deploys the concept “cell-free MIMO” for the 6G networks.

On the other hand, the paradigm of physical-layer network coding (PNC) has been examined in [7] as a way to apply network coding at the physical layer. The main idea of PNC is based on exploiting the interference between users under certain conditions rather than treating it as a destructive effect. A relay node transforms the received signals simultaneously to an interpretable form as output signals. The output signals are relayed to terminal nodes, i.e., their final destinations. The terminal nodes are extracted the necessary information from the relayed signals. In this way, the PNC scheme exploits the interference through simultaneously transmitted signals from different nodes for mapping the superposition of signals. Thus, in a two-way relay channel, two terminal nodes simultaneously transmit their own signals to the relay node in the first time slot. The relay node receives a superposition of two signals and decodes the network-coded symbol (NCS), i.e., $s_1 \oplus s_2$. Then, the relay broadcasts the decoded NCS to the terminal nodes in the second time slot. Finally, each terminal node retrieves the information symbol of the other terminal node by doing an XOR operation.

In the literature, the MIMO-based PNC has been examined in [8] by employing a linear MIMO detection scheme, i.e., log-likelihood ratio (LLR). In the PNC with multiple antennas, the relay node decodes the NCS by extracting the sum and difference of the two signals. Then, the authors of [9] have extended the PNC to the multi-user massive MIMO applications. Nevertheless, the PNC scheme has yet to be applied to multiple relay nodes that jointly decode the NCS to the best of our knowledge.

Addressing the above-mentioned gap in the literature, in this paper, we propose a novel scheme for PNC-based cell-free MIMO to improve reliability while reducing the trans-

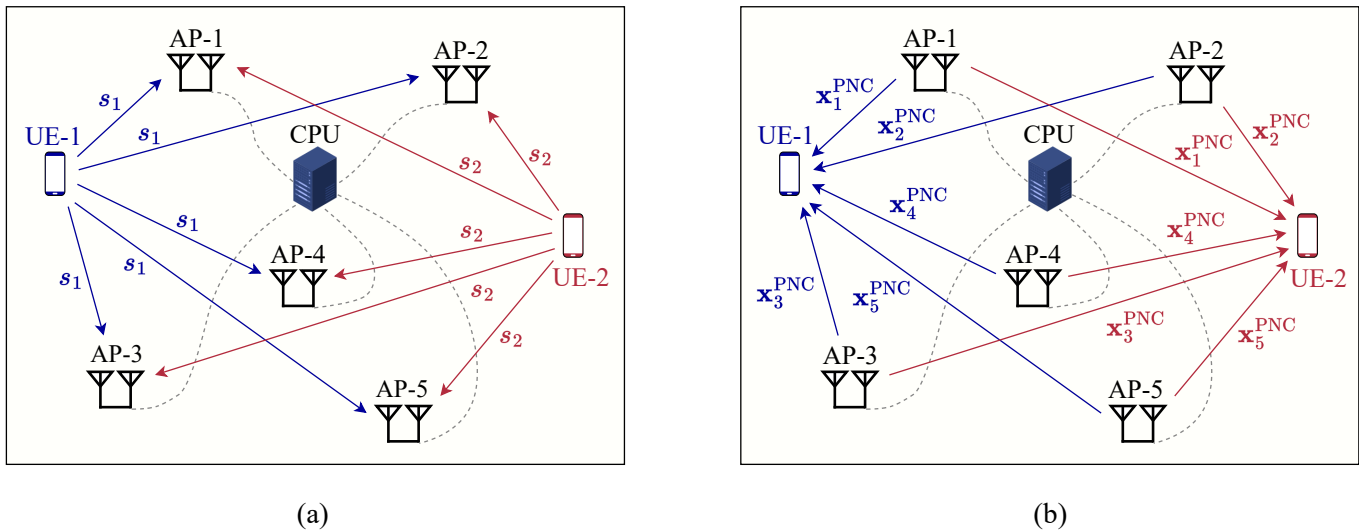


Figure 1: (a) Uplink transmission and (b) downlink transmission of the proposed PNC-based cell-free MIMO system.

mission delay. In this scheme, the APs are considered as relay nodes for all user pairs that need to exchange their data simultaneously. Similarly, the user equipments (UEs) in the coverage area are regarded as the terminal nodes. Then, the data exchange between UEs is accomplished in two time slots by exploiting the PNC instead of four time slots. Hence, the delay in transmission is significantly reduced. Furthermore, we show that the proposed scheme considerably outperforms the conventional cell-free MIMO system regarding the bit error rate (BER).

Notation. Matrices are indicated by uppercase bold letters while vectors are represented by lowercase bold letters. Mathematical operations, including inversion, transpose, conjugate transpose, absolute value, trace, and expectation, are represented by $(\cdot)^{-1}$, $(\cdot)^T$, $(\cdot)^H$, $|\cdot|$, $\text{tr}(\cdot)$, and $\mathbb{E}\{\cdot\}$, respectively. The complex number field is denoted by \mathbb{C} . The $n \times n$ identity matrix is represented by \mathbf{I}_n , while the $n \times 1$ zero vector is denoted by $\mathbf{0}_n$. Moreover, $\mathcal{CN}(0, \sigma^2)$ stands for a complex Gaussian random variable with zero mean and variance σ^2 .

Organization. This paper is organized as follows. In Section II, the system model of the proposed PNC-based cell-free MIMO and the detection schemes of the conventional cell-free MIMO system are given. Section III provides the detection schemes for the proposed PNC-based cell-free MIMO. In Section IV, the simulation results are provided in terms of the end-to-end bit error rate. In Section V, the conclusion of the paper is presented with future work.

II. SYSTEM MODEL

We consider a PNC-based cell-free MIMO system including M randomly distributed APs, each equipped with N antennas, K randomly distributed single-antenna UEs, and a central processing unit (CPU). The system contains $Q = K/2$ user pairs where K is an even integer. Also, the total number of antennas is much bigger than the number of users, i.e., $MN \gg K$ where $N \geq K$. All APs are connected to the CPU,

which coordinates the APs via fronthaul links, and they are cooperatively serving each active UE through coherent joint transmission and reception.

We perform the uplink transmission and downlink transmission sequentially for the considered cell-free MIMO system utilizing time division duplexing (TDD) to achieve end-to-end data transmission. Figure 1(a) demonstrates the uplink transmission of the proposed PNC-based cell-free MIMO system for 5 APs with 2 antennas and 2 single-antenna UEs while Figure 1(b) shows the downlink transmission. For the sake of simplicity, we assume that the perfect local channel state information (CSI) is available at the APs. Moreover, without loss of generality, binary phase-shift keying (BPSK) is utilized as the modulation scheme for all users in both conventional and PNC-based cell-free MIMO systems. Notably, the proposed PNC-based cell-free MIMO employs the same modulation scheme for each user in the same pair.

A. Detection Schemes for Conventional Cell-Free MIMO

In this subsection, we present a conventional cell-free MIMO system that performs end-to-end data transmission, comprising both uplink and downlink transmission phases in four time slots.

1) *Uplink Transmission:* In the uplink transmission of a cell-free MIMO network, all APs receive a superposition of the signals sent by all UEs. Therefore, the received signal at the m^{th} AP is defined as [3]

$$\mathbf{y}_m^{\text{UL}} = \sum_{i=1}^K \mathbf{h}_{m,i} s_i + \mathbf{n}_m, \quad (1)$$

where $s_i \in \mathbb{C}$ is the signal transmitted by the i^{th} UE with the power $p_i = \mathbb{E}\{|s_i|^2\}$, and $\mathbf{n}_m \sim \mathcal{CN}(\mathbf{0}_N, \sigma_{\text{UL}}^2 \mathbf{I}_N)$ is the receiver noise. The channel vector for m^{th} AP and k^{th} UE,

$\mathbf{h}_{m,k} \in \mathbb{C}^{N \times 1}$ is defined by an uncorrelated Rayleigh fading, which is

$$\mathbf{h}_{m,k} \sim \mathcal{CN}(\mathbf{0}_N, \beta_{m,k} \mathbf{I}_N), \quad (2)$$

where $\beta_{m,k}$ describes the large-scale fading coefficient.

In order to decode the information from the received signal, the m^{th} AP can compute an estimate of the signal s_k transmitted by the k^{th} UE. This estimate is denoted by $\hat{s}_{m,k}$. For this purpose, the m^{th} AP needs to use a receive combining vector $\mathbf{v}_{m,k} \in \mathbb{C}^{N \times 1}$. Thus, the estimate $\hat{s}_{m,k}$ can be defined as

$$\hat{s}_{m,k} = \mathbf{v}_{m,k}^H \mathbf{y}_m^{\text{UL}}. \quad (3)$$

The receive combining vectors are determined based on the zero-forcing (ZF) combining matrix, which is defined at the m^{th} AP as

$$\mathbf{V}_m = \mathbf{H}_m (\mathbf{H}_m^H \mathbf{H}_m)^{-1}, \quad (4)$$

where $\mathbf{H}_m = [\mathbf{h}_{m,1}, \mathbf{h}_{m,2}, \dots, \mathbf{h}_{m,K}] \in \mathbb{C}^{N \times K}$ is the composite channel matrix associated with the m^{th} AP and $\mathbf{V}_m = [\mathbf{v}_{m,1}, \mathbf{v}_{m,2}, \dots, \mathbf{v}_{m,K}] \in \mathbb{C}^{N \times K}$.

By substituting (1) in (3), it can be written as follows

$$\hat{s}_{m,k} = \mathbf{v}_{m,k}^H \mathbf{h}_{m,k} s_k + \sum_{\substack{i=1 \\ i \neq k}}^K \mathbf{v}_{m,k}^H \mathbf{h}_{m,i} s_i + \mathbf{v}_{m,k}^H \mathbf{n}_m. \quad (5)$$

The implementation of uplink transmission is characterized by different degrees of cooperation among APs as centralized, distributed, and semi-distributed. Since we consider the semi-distributed implementation, the receive combining is performed at each AP by using the local CSI knowledge. On the other hand, data detection is performed by the CPU. All APs send their data estimates to the associated CPU, and the CPU gathers the local estimates of the data signals to compute its estimate such that

$$\hat{s}_k^{\text{CF}} = \sum_{m=1}^M \hat{s}_{m,k}. \quad (6)$$

Then, the maximum likelihood (ML) detection of the BPSK symbols \tilde{s}_k^{CF} are determined through \hat{s}_k^{CF} for $k = 1, 2, \dots, K$ based on the following

$$\tilde{s}_k^{\text{CF}} = \begin{cases} +1, & \hat{s}_k^{\text{CF}} \geq 0 \\ -1, & \hat{s}_k^{\text{CF}} < 0 \end{cases}. \quad (7)$$

2) *Downlink Transmission:* After the uplink transmission where the data signal of the k^{th} UE is detected by the CPU, the m^{th} AP transmits the signal $\mathbf{x}_m \in \mathbb{C}^{N \times 1}$ to all UEs in the downlink transmission of a cell-free MIMO network. Then, the received signal at the k^{th} UE is defined by

$$\mathbf{y}_k^{\text{DL}} = \sum_{m=1}^M \mathbf{h}_{m,k}^H \mathbf{x}_m + n_k, \quad (8)$$

where the receiver noise is $n_k \sim \mathcal{CN}(0, \sigma_{\text{DL}}^2)$. The signal transmitted by the m^{th} AP is formed by the precoded data signals belonging to different UEs. Therefore, it can be written

as

$$\mathbf{x}_m = \sum_{i=1}^K \mathbf{w}_{m,i} \zeta_i, \quad (9)$$

where ζ_k is the data signal for the k^{th} UE and $\mathbf{w}_{m,k} \in \mathbb{C}^{N \times 1}$ represents the local precoding vector assigned by the m^{th} AP for the data of the k^{th} UE. To accomplish the end-to-end data transmission, the data signal for the k^{th} UE will be $\zeta_k = \tilde{s}_k^{\text{CF}}$ with the power $p_k^{\text{CF}} = \mathbb{E}\{|\zeta_k|^2\}$. Then, the local precoding vector $\mathbf{w}_{m,k}$ is designed based on the local CSI available at the m^{th} AP. Thus, the ZF precoding matrix is calculated by

$$\mathbf{W}_m = \alpha \mathbf{H}_m (\mathbf{H}_m^H \mathbf{H}_m)^{-1}, \quad (10)$$

where $\mathbf{W}_m = [\mathbf{w}_{m,1}, \mathbf{w}_{m,2}, \dots, \mathbf{w}_{m,K}] \in \mathbb{C}^{N \times K}$ and α is the scaling factor with the following expression

$$\alpha = \frac{1}{\sqrt{\text{tr}((\mathbf{H}_m^H \mathbf{H}_m)^{-1})}}. \quad (11)$$

III. DETECTION SCHEMES FOR THE PROPOSED PNC-BASED CELL-FREE MIMO

This section presents a PNC-based cell-free MIMO system that accomplishes end-to-end data transmission through the uplink and downlink transmission phases in two time slots.

A. Uplink Transmission

For the proposed PNC-based cell-free MIMO system, the received signal at the m^{th} AP is rewritten as [8]

$$\mathbf{y}_m^{\text{PNC}} = \mathbf{H}_m \mathbf{D}^{-1} \mathbf{D} \mathbf{s} + \mathbf{n}_m, \quad (12)$$

where $\mathbf{s} = [s_1, s_2, \dots, s_K]^T \in \mathbb{C}^{K \times 1}$ is the transmitted signal vector for the m^{th} AP with the power $p_k = \mathbb{E}\{|s_k|^2\}$ for $k = 1, 2, \dots, K$, and \mathbf{D} represents the sum-difference matrix which is defined by

$$\mathbf{D} = \begin{bmatrix} \mathbf{I}_Q & \mathbf{I}_Q \\ \mathbf{I}_Q & -\mathbf{I}_Q \end{bmatrix}_{K \times K}. \quad (13)$$

Then, the received signal in (12) can be redefined by the following equation

$$\mathbf{y}_m^{\text{PNC}} = \bar{\mathbf{H}}_m \bar{\mathbf{s}} + \mathbf{n}_m, \quad (14)$$

where $\bar{\mathbf{H}}_m = \mathbf{H}_m \mathbf{D}^{-1}$ is the reformed composite channel matrix and $\bar{\mathbf{s}} = \mathbf{D} \mathbf{s}$ is the reformed transmitted signal vector such that

$$\bar{\mathbf{s}} = \begin{bmatrix} s_1 + s_{Q+1} \\ s_2 + s_{Q+2} \\ \vdots \\ s_Q + s_{2Q} \\ s_1 - s_{Q+1} \\ s_2 - s_{Q+2} \\ \vdots \\ s_Q - s_{2Q} \end{bmatrix}_{K \times 1}. \quad (15)$$

The received signal vector after the receive combining is expressed by the following expression

$$\mathbf{r}_m = \bar{\mathbf{V}}_m^H \mathbf{y}_m^{\text{PNC}}, \quad (16)$$

where $\mathbf{r}_m = [r_{m,1}, r_{m,2}, \dots, r_{m,K}]^T \in \mathbb{C}^{K \times 1}$ and the receive combining matrix $\bar{\mathbf{V}}_m \in \mathbb{C}^{N \times K}$ is computed over the reformed composite channel matrix $\bar{\mathbf{H}}_m$ by using the ZF combining such that

$$\bar{\mathbf{V}}_m = \bar{\mathbf{H}}_m \left(\bar{\mathbf{H}}_m^H \bar{\mathbf{H}}_m \right)^{-1}. \quad (17)$$

Then, we perform the log-likelihood ratio (LLR) based on the maximum a posteriori estimator to compute the local estimates of the PNC symbols at each AP. The LLR is defined in terms of the log-likelihood of the q^{th} and $(q+Q)^{\text{th}}$ symbols by the following equation [9]

$$\text{LLR}_{m,q} = \text{LL}_{m,q+Q} - \text{LL}_{m,q}, \quad (18)$$

where

$$\text{LL}_{m,q+Q} = \log \left(e^{\frac{2r_{m,q+Q} - 2}{\sigma_{m,q+Q}^2}} + e^{\frac{-2r_{m,q+Q} - 2}{\sigma_{m,q+Q}^2}} \right) \quad (19)$$

and

$$\text{LL}_{m,q} = \log \left(e^{\frac{2r_{m,q} - 2}{\sigma_{m,q}^2}} + e^{\frac{-2r_{m,q} - 2}{\sigma_{m,q}^2}} \right). \quad (20)$$

where $\sigma_{m,q}^2$ and $\sigma_{m,q+Q}^2$ are the noise variances of the q^{th} and $(q+Q)^{\text{th}}$ symbol for the m^{th} AP after the combining operation, respectively. Then, the noise variances can be defined as

$$\sigma_{m,i}^2 = \left\{ \bar{\mathbf{V}}_m^H \bar{\mathbf{V}}_m \right\}_{i,i} \sigma_{\text{UL}}^2, \quad (21)$$

where $\{\cdot\}_{i,i}$ gives the i^{th} diagonal term for $i \in \{1, 2, \dots, 2Q\}$. Each AP sends its LLR value associated with the q^{th} user pair to the CPU. Then, the CPU computes the sum-LLR value by

$$\text{LLR}_q^{\text{sum}} = \sum_{m=1}^M \text{LLR}_{m,q}. \quad (22)$$

Finally, the CPU detects the PNC symbols for the case of BPSK modulation as:

$$\tilde{s}_q^{\text{PNC}} = \begin{cases} +1, & \text{LLR}_q^{\text{sum}} \geq 0 \\ -1, & \text{LLR}_q^{\text{sum}} < 0 \end{cases}, \quad (23)$$

where $q \in \{1, 2, \dots, Q\}$.

B. Downlink Transmission

In the downlink transmission of the PNC-based cell-free MIMO system, the m^{th} AP transmits the signal $\mathbf{x}_m^{\text{PNC}}$ to all UEs as shown in Figure 1(b).

Since the data signals for the q^{th} and $(q+Q)^{\text{th}}$ UEs are the same, which is \tilde{s}_q^{PNC} , the received signals of these users

can be defined by

$$\begin{aligned} y_q^{\text{PNC}} &= \sum_{m=1}^M \mathbf{h}_{m,q}^H \mathbf{x}_m^{\text{PNC}} + n_q, \\ y_{q+Q}^{\text{PNC}} &= \sum_{m=1}^M \mathbf{h}_{m,q+Q}^H \mathbf{x}_m^{\text{PNC}} + n_{q+Q}, \end{aligned} \quad (24)$$

where the noise terms are $n_q \sim \mathcal{CN}(0, \sigma_{\text{DL}}^2)$ and $n_{q+Q} \sim \mathcal{CN}(0, \sigma_{\text{DL}}^2)$.

Then, the precoded data signal for the PNC is defined by

$$\mathbf{x}_m^{\text{PNC}} = \sum_{i=1}^K \mathbf{w}_{m,i} \xi_i, \quad (25)$$

where ξ_k is the data signal for the k^{th} UE and $\mathbf{w}_{m,k} \in \mathbb{C}^{N \times 1}$ is the local precoding vector calculated by using (10) and (11). For end-to-end data transmission, the data signals for the q^{th} and $(q+Q)^{\text{th}}$ UEs will be $\xi_q = \xi_{q+Q} = \tilde{s}_q^{\text{PNC}}$ with the power $p_{q+Q}^{\text{PNC}} = p_q^{\text{PNC}} = \mathbb{E}\{|\xi_q|^2\}$ for $q \in \{1, 2, \dots, Q\}$.

The only difference of the PNC-based cell-free MIMO in downlink transmission compared to the conventional scheme is that all APs transmit the same PNC signal to the users in the same pair. Then, when BPSK is used for modulation, the decoded bits at the q^{th} UE and the $(q+Q)^{\text{th}}$ UE are determined [10] respectively by

$$\hat{b}_q^R = \begin{cases} 1, & \text{Re}(y_q^{\text{PNC}}) \geq 0 \\ 0, & \text{Re}(y_q^{\text{PNC}}) < 0 \end{cases}, \quad (26)$$

and

$$\hat{b}_{q+Q}^R = \begin{cases} 1, & \text{Re}(y_{q+Q}^{\text{PNC}}) \geq 0 \\ 0, & \text{Re}(y_{q+Q}^{\text{PNC}}) < 0 \end{cases}. \quad (27)$$

Each user obtains the transmitted data of the other user in the same pair through XOR operation by using its own data bits and the decoded data bits.

In the q^{th} pair, the q^{th} UE determines the data of the $(q+Q)^{\text{th}}$ UE, i.e., \tilde{b}_{q+Q} , by using its own data b_q such that

$$\tilde{b}_{q+Q} = b_q \oplus \hat{b}_q^R. \quad (28)$$

Similarly, the $(q+Q)^{\text{th}}$ UE determines the data of the q^{th} UE, i.e., \tilde{b}_q , by using its own data b_{q+Q} such that

$$\tilde{b}_q = b_{q+Q} \oplus \hat{b}_{q+Q}^R. \quad (29)$$

Hence, the q^{th} UE obtains \tilde{b}_{q+Q} while the $(q+Q)^{\text{th}}$ UE obtains \tilde{b}_q , which results in exchanging the data bits belonging to two users in two time slots.

IV. SIMULATION RESULTS

In this section, we provide the simulation results of the proposed PNC-based cell-free MIMO system compared to the conventional cell-free MIMO system. We hereby deploy the cell-free MIMO system in an urban environment with a total coverage area of $500 \text{ m} \times 500 \text{ m}$. For the network deployment, the APs are uniformly distributed within the coverage area such that they are at least 50 meters away from each other

[11]. In addition, the height difference between each AP and each UE is 10 meters in order to be coherent to the 3GPP urban microcell model defined by [12].

In the urban microcell model for sub-6 GHz frequency bands, the large-scale fading coefficient in (2) is characterized by the log-distance path-loss model with uncorrelated shadow fading and computed by [3]

$$\beta_{m,k}[\text{dB}] = -20 \log_{10} \left(\frac{4\pi d_0}{\lambda} \right) - 10\gamma \log_{10} \left(\frac{d_{m,k}}{d_0} \right) + F_{m,k}, \quad (30)$$

where d_0 is the reference distance, $\lambda = c/f_c$ is the carrier wavelength, c is the speed of light, f_c is the carrier frequency, γ is the path-loss exponent, $d_{m,k}$ is the distance between m^{th} AP and k^{th} UE, and $F_{m,k} \sim \mathcal{N}(0, \sigma_{sh}^2)$ is the shadow fading with a mean 0 dB and a standard deviation σ_{sh} in dB. Moreover, the noise powers in the uplink and downlink transmissions are calculated by $\sigma_{UL}^2 = \sigma_{DL}^2 = N_0 B$ where N_0 is the noise spectral density in W/Hz and B is the bandwidth in Hz.

In the uplink transmission, the power of the signal transmitted by each UE is equal to the maximum uplink transmit power, i.e., $p_k = P_{ul}$ for $k = 1, 2, \dots, K$. In the downlink transmission, the total downlink transmit power P_{dl} is equally shared among all UEs such that $p_k^{\text{PNC}} = p_k^{\text{CF}} = P_{dl}/K$ for both conventional and proposed cell-free MIMO schemes. The simulation parameters are then given in Table I.

The performance results are given as the probability of having a bit error rate (BER) that is lower than a given threshold value BER_{th} , i.e., $\Pr\{\text{BER} < \text{BER}_{th}\}$. Here, BER is the average bit error rate of the users in the same pair.

In Figure 2, we compare end-to-end BER performances of the proposed PNC-based cell-free MIMO and the conventional cell-free MIMO schemes in the same network deployment, including 5 randomly distributed APs. It is shown that the proposed scheme facilitates a less erroneous transmission compared to the conventional cell-free MIMO system, which means that the PNC-based cell-free MIMO enables more

Table I: Simulation parameters.

Parameter	Value
Coverage area	500 m \times 500 m
Number of APs, M	5 or 9
Number of antennas per AP, N	2
Number of UEs, K	2
Number of user pairs, Q	1
Carrier frequency, f_c	2.4 GHz
Bandwidth, B	1 MHz
Maximum uplink transmit power, P_{ul}	20 dBm
Total downlink transmit power, P_{dl}	30 dBm
Noise spectral density, N_0	-174 dBm/Hz
Path-loss exponent, γ	3.67
Reference distance, d_0	1 m
Standard deviation, σ_{sh}	4

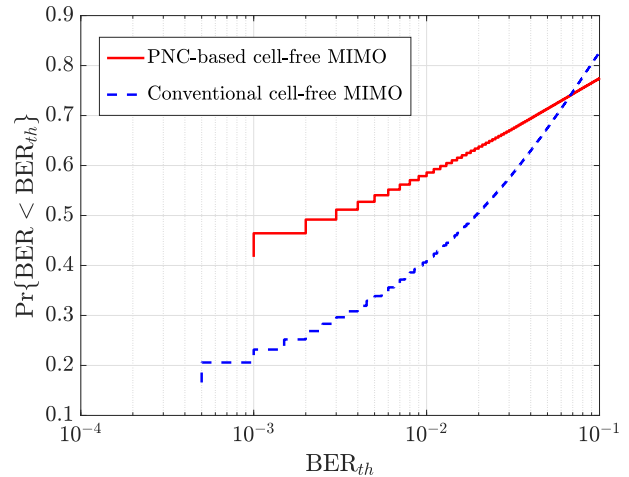


Figure 2: End-to-end BER comparison for the cell-free MIMO network with 5 APs.

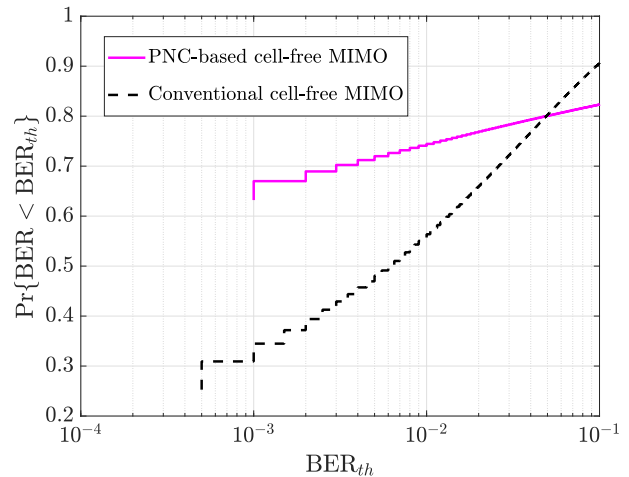


Figure 3: End-to-end BER comparison for the cell-free MIMO network with 9 APs.

reliable transmission while reducing the transmission delay. Specifically, the probability of achieving a BER less than 10^{-2} is approximately 0.6 for the proposed scheme, while it is only 0.4 for the conventional scheme, as depicted in the Figure 2. This implies that the PNC-based cell-free MIMO scheme offers a more reliable transmission.

In Figure 3, the cell-free MIMO network comprises 9 randomly distributed APs. For this deployment, the PNC-based cell-free MIMO outperforms the conventional scheme while reducing the transmission delay. The results show that the conventional scheme can reach a BER of less than 10^{-3} with a probability of 0.3 while the proposed PNC-based scheme can have a probability of 0.65. Thus, the results confirm the effectiveness of the PNC-based scheme in densely deployed networks regarding the BER performance.

V. CONCLUSION

This paper proposes the novel PNC-based cell-free MIMO for 6G wireless networks. The proposed scheme utilizes the PNC in the cell-free MIMO network where a higher number of APs are cooperatively serving a smaller number of UEs in the same time and frequency band. The PNC-based scheme transforms the received superimposed signals into an NCS. Thus, interference does not act as a limiting factor in PNC. In addition, the transmission delay is decreased since the required number of time slots for end-to-end communication is reduced. The performance evaluations are acquired in terms of BER and show that the proposed scheme achieves considerably less BER. In other words, the proposed PNC-based cell-free MIMO scheme enables more reliable transmission compared to conventional cell-free MIMO networks while reducing the transmission delay. In future work, different modulation schemes and LLR combining strategies will be examined to further improve the performance of the PNC-based cell-free MIMO networks.

ACKNOWLEDGMENT

This work has been partially funded by the European Union Horizon 2020. RISE 2018 scheme (H2020-MSCA-RISE-2018) under the Marie Skłodowska-Curie grant agreement No. 823903 (RECENT).

REFERENCES

- [1] H. Q. Ngo, A. Ashikhmin, H. Yang, E. G. Larsson, and T. L. Marzetta, "Cell-Free Massive MIMO: Uniformly Great Service for Everyone," in *Proc. IEEE International Workshop on Signal Processing Advances in Wireless Communications (SPAWC)*, pp. 201-205, 2015.
- [2] E. Nayebi, A. Ashikhmin, T. L. Marzetta, and H. Yang, "Cell-Free Massive MIMO systems," in *Proc. Asilomar Conference on Signals, Systems and Computers*, pp. 695-699, 2015.
- [3] Ö. T. Demir, E. Björnson, and L. Sanguinetti, "Foundations of User-Centric Cell-Free Massive MIMO," *Foundations and Trends® in Signal Processing*, vol. 14, no. 3-4, pp 162-472, 2021.
- [4] H. Q. Ngo, A. Ashikhmin, H. Yang, E. G. Larsson, and T. L. Marzetta, "Cell-Free Massive MIMO Versus Small Cells," *IEEE Transactions on Wireless Communications*, vol. 16, no. 3, pp. 1834-1850, Mar. 2017.
- [5] H. I. Obakhena, A. L. Imoize, F.I. Anyasi, and K. V. N. Kavitha, "Application of Cell-Free Massive MIMO in 5G and Beyond 5G Wireless Networks: A Survey," *Journal of Engineering and Applied Science*, vol. 68, no. 13, Oct. 2021.
- [6] H. A. Ammar, R. Adve, S. Shahbazpanahi, G. Boudreau, and K. V. Srinivas, "User-Centric Cell-Free Massive MIMO Networks: A Survey of Opportunities, Challenges and Solutions," *IEEE Communications Surveys & Tutorials*, vol. 24, no. 1, pp. 611-652, Firstquarter 2022.
- [7] S. Zhang, S. C. Liew, and P. P. Lam "Hot Topic: Physical-layer Network Coding," in *Proc. ACM/IEEE International Conference on Mobile Computing and Networking*, pp. 358-365, Sept. 2006.
- [8] S. Zhang and S. C. Liew, "Physical Layer Network Coding with Multiple Antennas," in *Proc. IEEE Wireless Communication and Networking Conference (WCNC)*, pp. 1-6, 2010.
- [9] B. Okyere, L. Musavian, and R. Mumtaz, "Multi-User Massive MIMO and Physical Layer Network Coding," in *Proc. IEEE Globecom Workshops*, pp. 1-6, 2019.
- [10] J. G. Proakis and M. Salehi, *Digital Communications*, 5th ed. New York, NY, USA: McGraw-Hill, 2007.
- [11] E. Björnson and L. Sanguinetti, "Cell-Free versus Cellular Massive MIMO: What Processing is Needed for Cell-Free to Win?," in *Proc. IEEE International Workshop on Signal Processing Advances in Wireless Communications (SPAWC)*, pp. 1-5, 2019.
- [12] 3GPP, *Further Advancements for E-UTRA Physical Layer Aspects (Release 9)*. 3GPP TS 36.814, Mar. 2017.